Separation and Purification Technology 150 (2015) 1–12

Contents lists available at ScienceDirect

Separation and Purification Technology

journal homepage: www.elsevier.com/locate/seppur

Effect of Mg^{2+} binding on transmission of bovine serum albumin (BSA) through ultrafiltration membranes

Laura T. Rodríguez Furlán, Mercedes E. Campderrós *

Instituto de Investigaciones en Tecnología Química (INTEQUI-CONICET-CCT San Luis), Facultad de Química, Bioquímica y Farmacia, Universidad Nacional de San Luis, Ejército de los Andes 950, 5700 San Luis, Argentina

ARTICLE INFO

Article history:
Received 29 March 2015
Received in revised form 16 June 2015
Accepted 17 June 2015
Available online 18 June 2015

Keywords:
Ultrafiltration
BSA
Transmission
Protein fractionation

ABSTRACT

Protein fractionation by membrane technology has many advantages for separations, in comparison with conventional methods. In this paper, the influence of different type and concentration of two electrolytes: NaCl and $MgCl_2$ on buffer capacity and hydrodynamic radius of bovine plasma proteins were analyzed as a way to improve protein separation by cross-flow ultrafiltration. A tubular ceramic membrane with 0.2 μm pore size was used. The evolution of permeate flux and BSA transmission was determined at 25 °C and transmembrane pressure range of 0.2–1.4 bar. The membrane fouling was evaluated through the resistance model application, identifying the operational conditions of the highest BSA transmission through the membrane. In this regard, it was demonstrated that the effective radius of the protein and its buffering capacity were affected by the use of $MgCl_2$ at 0.006 (w/v), which caused conformation changes in the protein structure resulting in a less resistance to transport.

1. Introduction

During the last decades, membranes attracted the attention of scientists due to their unique separation principle, i.e. the selective transport and efficient separation in comparison with other unit operations. Separations with membranes do not require additives, and they can be performed isothermally at low temperatures with less energy consumption compared to other thermal separation processes [1].

Among the membranes used in industry, the inorganic ones possess good mechanical, thermal and chemical resistance to solvent and oxidizers. This explains the growing interest in them, especially in the food industry [1,2]. In this regard, inorganic membranes have several advantages over polymeric membranes, such as narrower pore-size distribution and a better resistance to extreme pH and temperatures. Ultrafiltration (UF) with ceramic membranes is used in the recovery, separation and concentration of proteins in the biotechnological industry [1,3–10]. In these processes, protein retention is not only based on steric hindrance, but also on the chemical nature of the membrane and the physico-chemical environment of the solute. In this respect, pH and ionic strength determine the electrostatic interactions between the membrane and the protein [3].

In order to perform the separation of protein mixture with UF membranes, it is important to consider the ratio of the protein molecular mass to be separated, the change of the physico-chemical environment, as well as the chemical modification of membranes. Thus, permeation or transmission of a charged protein through a membrane depends mostly on the electrostatic interactions between the proteins and the membrane, and the relationship between the protein size and the membrane pore size. Transmission also depends on the physico-chemical environment of the solute, and on the chemical nature of the membrane [5,7].

Bovine plasma is a suspension containing components of different molecular weights and proportions, among them, bovine serum albumin (BSA) is among the smallest (66.5 kDa), and it is present in a higher proportion (Table 1) [11]. In this regard, the application of membrane technology as separation method is a viable alternative.

The isolation of proteins is important from a technological point of view, since each protein exhibits its own functional properties which can be used in different applications as a food ingredient. Here, Chove et al. [12] and Mueller et al. [13] investigated the functional properties of the protein fractions of soy proteins, and linseed meal, obtained by microfiltration and precipitation, respectively, according to their pH solubility. They found that each protein fraction showed differences in their functional properties and may be selected for a given food formulation.

BSA solutions have numerous applications including protein concentration reference standards for use in bicinchoninic acid

* Corresponding author.
E-mail address: mcamp@unsl.edu.ar (M.E. Campderrós).

http://dx.doi.org/10.1016/j.seppur.2015.06.021
1383-5866/

Nomenclature

C_A	concentration of the base *B*, mol L^{-1}
C_B	concentration of the acid *A*, mol L^{-1}
c_i	concentration of each ion species, mol L^{-1}
C_P	concentration in the permeate, mol L^{-1}
C_R	concentration in the retentate, mol L^{-1}
e	electron charge (1.602176×10^{-19} C)
J_p	permeate flux ($m^3\ h^{-1}\ m^{-2}$)
J_w	pure water permeation fluxes ($m^3\ h^{-1}\ m^{-2}$)
k^{-1}	Debye length (m)
k_B	Boltzmann constant ($1.38 \times 10^{-23}\ m^2\ kg/s^2\ K$)
k_{eff}^{-1}	effective Debye length (m)
n_c	ion concentration for the monovalent cations
n_{eff}	effective concentration
n_p	ion concentration for the macroions
n_s	ion concentration for the monovalent anions
P_H	membrane hydraulic permeability (L/h m^2 bar)
R_F	resistance due to irreversible fouling (m^{-1})
R_P	resistance due to the polarization layer of the solute on the membrane surface (m^{-1})
R_M	resistance of the clean membrane (m^{-1})
R_S	fouling resistance due to the solute (m^{-1})
r_s	solute radius (m)
T	absolute temperature (K)
T_r	solute transmission
Z	number of charges per polyelectrolyte chain
z_i	oxidation state or number of electric charges of each ion species

Greek letters

ΔP	operation transmembrane pressure (Pa)
σ_S	surface charge density
α	parameter dependent on the mass transfer characteristics of the system
ε	dielectric constant of water
μ	dynamic viscosity of the permeate at 25 °C (kg/m s o Pa s)
λ	ratio between the solute and the pore radius of the membrane
β	buffer capacity
ε_0	permittivity of free space
ϕ_S	partition coefficient

Table 1
Characteristics of bovine plasma proteins (BPP).

Protein	Molecular weight (kDa)	Structure	Concentration (g/L)	Radius (nm)
BSA	66.5	Globular quaternary structure	45–50	4.1
α1-globuline	41–70	Fibrous A Helix secondary structure	2–4	3.4–4.2
α2-globuline	150–850	Fibrous A Helix secondary structure	4–7	5.6–11.1
β-globuline	80	Fibrous B pleated sheet secondary structure	7–10	4.4
γ-globuline	140	Globular quaternary structure	10–13	5.5
Fibrinogen	330	Fibrous quaternary structure	2–4	7.6

(BCA), Bradford and other protein assay protocols. BSA is the universally accepted reference protein for total protein quantitation [14]. It is also used in numerous biochemical applications including Enzyme Linked Immunosorbent Assays (ELISAs), immunoblots and immunohistochemistry [15]. Furthermore, BSA is used as a protectant agent in cell culture media for production of vaccines and for biotechnology applications [16,17].

Now, the separations of proteins by membrane technology are not a simple task and, to improve the effectiveness of the method, some special properties of these macromolecules are usually taken into account. Thus, it can be considered the fact that some ions join in a specific form to certain protein so the protein can fulfill a specific regulatory function. Such is the case of the BSA in bovine plasma; this binding produces changes in the shape of the protein space. Divalent ions such as calcium are actively involved in regulating cellular functions; while monovalent ions such as chloride, potassium or sodium, possessing a single electrical load, have a rather weak protein binding. Magnesium is a divalent ion with a smaller ionic radius in relation to calcium so, at its junction with proteins, it induces a formation of a more rigid conformation. In effect, the protein binding to Mg(II) causes a higher conformational change than that induced by Ca(II). However, the Mg(II) concentration should be 1000 times higher than the Ca(II) for binding to the specific sites of the BSA [18–20]. This conformational change may alter the effective hydrodynamic radius of the protein, and influence the transfer of proteins across the UF membranes.

In this regard, previous studies about binding or ligation of different ions to specific proteins sites of bovine serum albumin (BSA) and the conformational changes produced have been reported. Thus Liang et al. [21] studied the effect of ligation of Co(II) with human serum albumin (HSA) or BSA, where this interaction induces a conformational transition; Yongqia et al. [22] found a series of interactions between the Ni(II) ion and BSA, where a conformational change after the union of both was generated. However, there are few backgrounds for studies of binding of Mg(II) at specific sites of BSA that take into account the conformational changes resulting from the ligation of both, and how these changes influence their interactions with the surrounding environment because of the physico-chemical processes involved. Therefore, in this study we sought to investigate the effect of ligation of the Mg(II) ions at a determined concentration on protein conformation of BSA and possible physicochemical changes generated from this interaction. However, it considers that this interaction may be influenced by conditions and medium composition. Therefore, we studied the effect of the presence of ions Mg(II) and Na upon binding properties and the induced changes in BSA conformation as function of pH. The BSA conformation changes would make a difference in its interaction with the environment and therefore it can be concentrated in the retentate stream during ultrafiltration process, improving the separative process from the others plasma components.

2. Theory

2.1. Buffer capacity of bovine plasma proteins

As previously described, the major protein of the bovine plasma is the BSA, which is constituted by 20 essential amino acids with a

structure containing 583 units. The structure and properties of BSA in solution is characterized by a versatile conformation, dependent on the pH, ionic strength and presence of ions, among other factors [20]. According to Nakamura et al. [23], the conformation of BSA as a function of pH is classified as follows: conformer E, at pH 2.7; F at pH 3.8; N, at pH 5.3; A → B at pH 8.

It has been shown that the BSA conformation N has a compressed globular structure with a triangular core. The transition N → F occurs as a sharp expansion at pH between 4.4 and 3.8 (40–129 Å) [24]. The F → E transition is found in the pH range between 3.6 and 2.8, which has an expanded form (21–250 Å) [25].

Amino acids have one or more cationic and anionic groups and a side chain that may be ionized. In this regard, amino acids can act as buffers in aqueous solution; that is, the buffer capacity of a given substance is its resistance to pH changes, when a strong acid or base is added.

The effects of the buffer capacity in an electrolyte solution are defined as:

$$\beta = \frac{dC_B}{dpH} \quad \text{or} \quad \beta = -\frac{dC_A}{dpH} \tag{1}$$

where C_B and C_A represents the added concentrations (in equivalent) of the base B and acid A. The buffer capacity is a nonlinear function and is, simply, the inverse of the slope of the titration curve (β = 1/slope).

Fig. 1 shows the BSA buffer effect at different pH values and different conformations, and the pH at which the structural transitions occur [26].

2.2. Influence of the variation of the electrostatic medium in the hydrodynamic radius of protein (BSA)

A Debye sphere is a volume in which there is a sphere of influence, and outside of which the charges are shielded by the formation of an electrical double layer. An electrical double layer is a structure that appears on the surface of an object (solid particle, gas bubble, liquid drop, or porous body) when it is exposed to a fluid. The surface charge (either positive or negative), comprises ions adsorbed onto the object due to chemical interactions. The second layer is composed of ions attracted to the surface due to electrostatic interactions.

The double-layer is usually presented in systems formed by colloidal particles dispersed in a medium containing free charges or ions, whose electrostatic interactions depend on these free charges, causing the formation of the electrical double layer. The effective hydrodynamic volume or effective hydrodynamic radius of charged protein (colloid) is increased by the presence of an electrical double layer, which thickness is expressed by the Debye length, k^{-1} [27]. In this sense, the Debye length is a crucial parameter in the description of aqueous systems that include ions, charged colloids, surfactants, polyelectrolytes, and biopolymers. For this type of colloidal system, the Debye length, k^{-1}, is given by [28]:

$$k^{-1} = \left(\frac{\varepsilon\varepsilon_0 k_B T}{\sum c_i z_i^2 e^2}\right)^{1/2} \tag{2}$$

where k_B is the Boltzmann constant, c_i and z_i are the concentration and the oxidation state or number of electric charges of each ion species, T is the absolute temperature, e is the electron charge, ε is the dielectric constant of water, and ε_0 is the permittivity of free space.

In the case of a salt concentration equal to "zero" the Debye length depend on the concentration and charge of the solute particles in the solvent. If considering the bulk solution and a dilute protein solution, the separation between proteins and between the proteins and the membrane surface becomes so large that the double layer contribution to the net force is negligible. So for a dilute protein solution the interactions between the different proteins can be considered negligible. Thus, to calculate the Debye length (Eq. (2)) the magnitude should be used is the effective concentration (n_{eff}):

$$k_{eff}^{-1} = \left(\frac{\varepsilon\varepsilon_0 k_B T}{2 n_{eff} e^2}\right)^{1/2} \tag{3}$$

Debye length for a monovalent electrolyte solution (z_i = 1), can be expressed by:

$$k^{-1} = \left(\frac{\varepsilon\varepsilon_0 k_B T}{2 n_s e^2}\right)^{1/2} \tag{4}$$

The system is in contact with a bulk reservoir with given ion concentrations: n_s for the monovalent anions (n_s was experimentally obtained for each pH studied). If assumed that each polymer chain in solution corresponds to Z monovalent ions, Eq. (3) can be rewritten as:

$$k_{eff}^{-1} = \left(\frac{\varepsilon\varepsilon_0 k_B T}{2 n_c e^2}\right)^{1/2} \tag{5}$$

The system is in contact with a bulk reservoir with given ion concentrations: n_s for the monovalent anions, n_c for the monovalent cations and n_p for the macroions (the concentration of the polymer or protein). Therefore:

$$n_c = n_s + Z n_p \tag{6}$$

where Z is the number of elementary charges per polyelectrolyte chain.

Replacing Eqs. (6) in (5) and working with the equation of Debye length for a system consisting of a saline solution containing polymer it can be obtained the following equation:

$$k_{eff}^{-1} = \left(\frac{n_s}{n_s + Z n_p}\right)^{1/4} k^{-1} \tag{7}$$

where k^{-1} is the Debye length in pure salt solution (n_p = 0).

This equation shows that addition of a polyelectrolyte of concentration n_p and charge Z to an monovalent salt solution of concentration n_s changes the Debye length from k^{-1} to ${k_{eff}}^{-1}$. In terms of molar concentrations for n_s and n_p, Eq. (7) may be written as:

$$k_{eff}^{-1} = \frac{0.304}{\sqrt[4]{n_s(n_s + Z n_p)}}\text{nm} \tag{8}$$

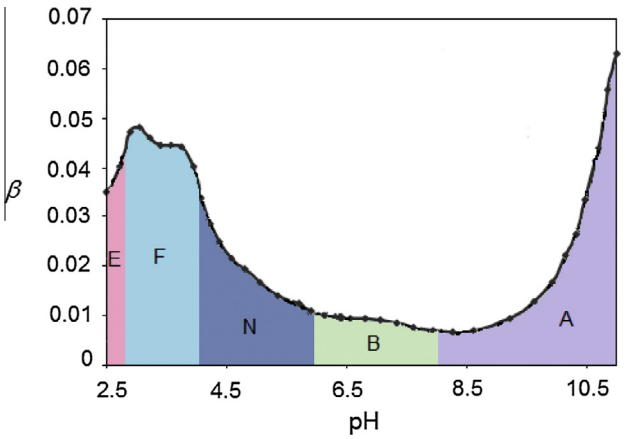

Fig. 1. Buffer capacity of BSA solution at different pH [26].

When the pH of a solution is adjusted, the ionic strength changed due to the concentration of acid or alkali. Thus, the Debye length can be calculated as a function of pH. Debye length is influenced by the pH, solute concentration and the protein–protein interactions. However, when working at a constant concentration (0.1% w/v) and with dilute solutions of bovine plasma (<0.2%, w/v) it can be considered that the interaction between the protein molecules are negligible and thus can observed as the pH influence on the Debye length (conductometric titration).

Pujar and Zydney [29] studied the protein separation by membrane ultrafiltration as a combination of steric and long-range (electrostatic) interactions between the protein and the porous surface of membrane. In this way, effective solute radius is expressed by:

$$r_{eff} = r_s + \frac{4r_s^3\sigma_s^2}{\varepsilon\varepsilon_0 k_B T}\lambda(1-\lambda)k_{eff}^{-1} \quad (9)$$

where r_s is the solute radius, σ_s surface charge density, λ is the ratio between the solute and the pore radius of the membrane, r_s/r_p.

The charge of a protein depends on the solution pH. Considering that the major protein of plasma is BSA (≅60%) with a radius r_s around of 4.1 nm (Table 1), a isoelectric point of 4.9 and a mean pore diameter of the membrane between 25 and 50 nm [30]. The surface charge density of BSA for each pH value can be calculated from the following equation developed by Smith and Deen [31] and used by de la Casa et al. [27] in colloidal systems:

$$\text{pH} \leqslant 4.9, \quad \sigma_S = 0.0145(4.9 - \text{pH}) \quad (10)$$

$$\text{pH} \geqslant 4.9, \quad \sigma_S = 0.0060(4.9 - \text{pH}) \quad (11)$$

Using these equations of the surface charge density is possible to obtain the effective radius of the solute as a function of pH (Eq. (9)).

The partition coefficient (ϕ_S) is defined as the ratio of concentrations of a substance in the retentate and permeate streams, and can be calculated from the expression given by de la Casa et al. [27], considering a membrane in which no clogging occurs during the run, the surface and the pore diameter of the membrane being maintained invariable during processing. For $\left(\frac{r_{eff}}{r_P}\right) \leqslant 1$:

$$\phi_S = \frac{\pi(r_P - r_{eff})^2}{\pi r_p^2} = \left(1 - \frac{r_{eff}}{r_P}\right)^2 = (1-\lambda_{eff})^2$$
$$\text{If } \left(\frac{r_{eff}}{r_P}\right) > 1, \quad \phi_S = 0 \quad (12)$$

This equation relates the effective radius of the protein at different pH values (r_{eff}, Eq. (9)) with the pore radius of the membrane (r_p). Therefore, the amount of solute that passes through the membrane from the feed to the permeate stream can be determined; it is the theoretical percentage of transmission ($T_{r\phi}$).

3. Materials and methods

3.1. Raw materials

The protein solutions used were prepared from bovine plasma protein (BPP) spray drying (Yerubá S.A., Argentina) base which comprised proteins of different molecular weight, radius and conformational structure (Table 1). The proximate composition provided by the manufacturer was: 76 ± 5% proteins, 0.1% fat, 10% ash, 4% water, 1% low molecular weight compounds. According to specifications provided by the supplier, BPP contained: Ca: 0.15 ± 0.02% (w/w) and Mg: 0.02 ± 0.005% (w/w). The BPP concentration was 0.1 ± 0.02 % (w/v). The solutions of NaCl and $MgCl_2$ (analytical grade) were prepared at different concentrations and pH. The pH values were adjusted with potassium hydroxide (KOH) and citric acid ($C_6H_8O_7$). The water used for the preparation of these solutions was treated by reverse osmosis (RO) with a conductivity <2 μS cm^{-1}.

The following determinations were performed in triplicate for each of the solutions tested.

3.2. Conductometric titration

Ions ligating protein produce a change of the protein net charge which causes a conformational change. In this regard, the proteins could present different net charge depending on the pH by binding to certain ions. The conductometric titration determines the conductivity of a solution through the loading of the species present, thus can be an indirect method to detect conformational changes in the protein by changes in the conductivity of the solution. Therefore the changes in protein conformation due to the presence of $MgCl_2$ and NaCl were analyzed by conductometric titration [32]. For this purpose, the following solutions were prepared: A: Plasma 0.1% (p/v); B: Plasma 0.1 % + $MgCl_2$ 0.006 % (p/v); C: Plasma 0.1 % + $MgCl_2$ 0.02 % (p/v); D: Plasma 0.1 % + NaCl 0.005 % (p/v); E: Plasma 0.1 % + $MgCl_2$ 0.006 % + NaCl 0.005 % (p/v); F: Plasma 0.1 % + $MgCl_2$ 0.006 % + NaCl 0.008 % (p/v); G: Plasma 0.1 % + $MgCl_2$ 0.006% + NaCl 0.02% (p/v). The pH was lowered to pH 2 with citric acid and, then, the protein solution was titled with 6 M KOH solution. The alkaline demand, pH (digital pH meter Altronix, Argentina), and the conductivity (digital conductivity meter Hanna Instruments, HI 9835, USA), were registered [33].

3.3. Permeation equipment

A mono-tubular mineral ultrafiltration (UF) membrane of 300 kDa MWCO, Carbosep M9 (Novasep Inc., USA) was tested in this work, with a mean pore diameter between 25 and 50 nm, a water flow of 72 L/h m^2 bar, to 25 °C. The membrane active layer consists of a thin deposit of ZrO_2–TiO_2 on a carbon porous support. The membrane length is 1.2 m and the inside diameter 6 mm, thus the membrane surface area is 0.025 m^2.

The assembly of the equipment used in the experiments is shown in Fig. 2. According to preliminary studies the tubular membrane module was fed at a constant speed (3.4 m min^{-1}) using a Masterflex Easy-Load pump model 7518–00. The retentate was recirculated to the feed tank while the permeate was collected. The transmembrane pressure, measured by a manometer, was held constant during the experiments (1.2 bar), with the help of a manual valve.

3.4. Membrane characterization

Fouling of MF/UF membrane during practical application for protein separation resulted from its adsorption on membrane surface significantly increases hydraulic resistance to flow, which

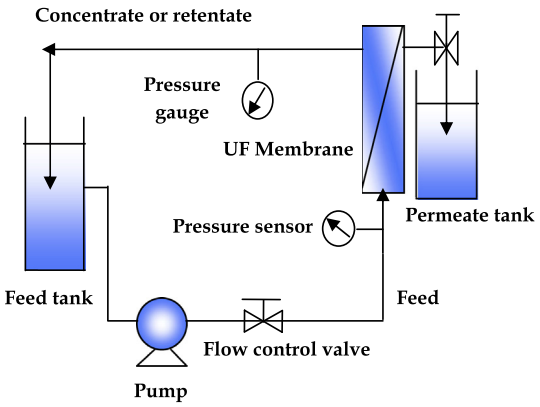

Fig. 2. Ultrafiltration equipment set-up.

reduced filtration flux rate and induced unfavorable effect on efficiency and economics of protein recovery processes [34]. So, it is necessary to assess the system performance that is permeate flux evolution and operating resistances. The membrane characterization was performed as described Diná Afonso et al. [8] with some modifications. At the beginning, the membrane was wetted out by circulating deionized water at 1.5 bar for 1 h. After this water permeated at pressures in the range of 0.2–1.4 bar in order to measure the corresponding water permeation fluxes, J_w, and determined the membrane hydraulic permeability, P_H:

$$J_w = P_H \cdot \Delta P \tag{13}$$

where ΔP is the operation transmembrane pressure.

From the slope the value of the hydraulic permeability is obtained.

The membrane resistances were calculated according to the resistances in series model [35] described as de la Casa et al. [3] for concentration of BSA through a tubular ceramic membrane. This model describes the permeate flux (J_p, $m^3\ h^{-1}\ m^{-2}$) in a filtration process as:

$$J_P = \frac{\Delta P}{\mu(R_M + R_S)} \tag{14}$$

where R_M and R_S are the hydraulic membrane resistance (m^{-1}) and the fouling resistance due to the solute (m^{-1}), respectively and μ is the dynamic viscosity of the permeate at 25 °C (kg/m s o Pa s).

R_M was determined recirculating water through the membrane at 25 °C at different values of transmembrane pressure. The measuring of permeate flow at each pressure value was made after steady state was reached. R_M was calculated as the inverse of the slope of the straight line that fits the data of water permeate flow against transmembrane pressure [36].

The resistance due to the solute can be calculated using the equation described by Ibanez et al. [36] who determined the resistance due to fouling in ceramic membranes to UF in a protein solution consisting of lysozyme and β-lactoglobulin at different values of transmembrane pressure

$$R_S = \frac{\Delta P}{\mu J_P} - R_M \tag{15}$$

where J_P is the density of final permeate flow or steady-state value for each pressure. The resistance due to solute fouling (R_S) is defined as follows:

$$R_S = R_F + R_P \tag{16}$$

where R_F is the resistance due to irreversible fouling formed from the physicochemical interaction of the membrane with the solute within the pores and on the surface of the membrane (m^{-1}); R_P is the resistance due to the polarization layer of the solute on the membrane surface (m^{-1}). Solute polarized layer on the surface of the membrane is a result of the applied pressure, therefore the R_P may be expressed as:

$$R_P = \alpha \Delta P \tag{17}$$

where α is a parameter dependent on the mass transfer characteristics of the system.

From Eqs. (16) and (17):

$$R_S = R_F + \alpha \Delta P \tag{18}$$

3.5. UF fractionation of bovine plasma: BSA separation

Feed solutions were prepared from bovine plasma powder, which was dissolved in deionized water at a concentration of 0.1 ± 0.01% (w/v) at its natural pH (7.25 ± 0.05), further solutions of bovine plasma in equal concentration with $MgCl_2$ in two concentrations (0.006 ± 0.0001 (%w/v) and 0.02 ± 0.001 % (w/v)) were prepared in order to study the influence of the salt concentration on the hydrodynamic radius of BSA. During UF, the retentate flow was recirculated to the feed tank under the following operating conditions: trans-membrane pressure 1.2 bar, cross-flow velocity 3.4 m min^{-1}, temperature 25 ± 1 °C, to obtain a VCR of 1.1. Samples of permeate and retentate were collected.

The cleaning of the fouled membrane was performed by applying a "Cleaning in Place" (CIP) procedure according to the manufacturer's instructions. At the end of each run, a cycle of water/alkali (NaOH, 0.1 M, 50 °C, 40 min)/water wash/NaOCl (300 ppm, 30 min)/water wash/HNO_3 0.1 M (20 °C 40 min)/water wash was applied to the membrane at a transmembrane pressure of 1 bar. Measurements of normalized water permeability were performed in order to verify the recovery of the flow through the membrane and the optimal performance during the separation process.

From the samples taken from both streams, the protein concentration was determined using the Bradford technique. Subsequently, the experimental solute transmission (T_r) was calculated as the relationship between its concentration in the permeate (C_P) and the concentration in the retentate (C_R) and the VCR, to compare with the data obtained from $T_{r\phi}$ expressed as a function of feed solution concentration:

$$T_r = \frac{[C_P/(C_P + C_R)] \times 100}{VCR} \tag{19}$$

3.6. SDS–PAGE electrophoresis

Polyacrylamide gel electrophoresis (SDS–PAGE) was carried out in a discontinuous buffer system: resolving gel buffer 1.5 M Tris–HCl, pH 8.8, stacking gel buffer 0.5 M Tris–HCl, pH 6.8, 10% (w/v) SDS. Sample buffer used was 62.5 mM tris–HCl, pH 6.8, 10% (v/v) glycerol, 2% (w/v) SDS, and 0.025% (w/v) bromophenol blue, 5% (v/v) 2-mercaptoethanol were added. The gel was prepared with 7% stacking gel and 4% resolving gel. Runs were performed in a vertical electrophoresis unit (Mini-Protean® 3 Cell, Bio-Rad, U.S.) at 75 V for 0.25 h, followed by 100 V for about 1.6 h, with electrode buffer (0.025 M Tris–HCl, 0.192 M glycine, and 0.1% (w/v) SDS, pH 8.3), until the tracking dye migrated to the bottom edge of the gel. Gels were stained with Cromassie Brilliant Blue R-250 (0.1% w/v) in methanol-acetic (40% (v/v)) and acid–water (10% (v/v)), and detained in the same solution without dye. The protein

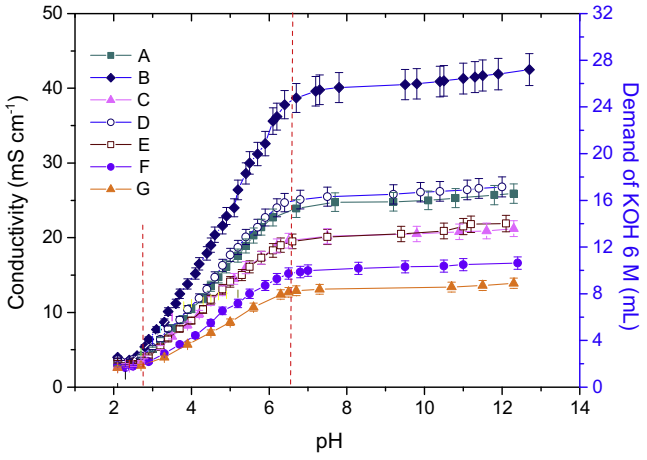

Fig. 3. Alkaline demand of the conductometric titration of bovine plasma proteins solutions at 0.1% (w/v) with different concentrations of $MgCl_2$ and NaCl. A: BPP; B: 0.1% BPP + 0.006% (w/v) $MgCl_2$; C: BPP + 0.02% (w/v) $MgCl_2$; D: BPP + 0.005% (w/v) NaCl; E: BPP + 0.006% (w/v) $MgCl_2$ + 0.005% (w/v) NaCl; F: BPP + 0.006% (w/v) $MgCl_2$ + 0.008% (w/v) NaCl; G: BPP + 0.006% (w/v) $MgCl_2$ + 0.02% (w/v) NaCl.

fractions were identified using molecular weight marker (SIGMA) (MW 30,000–200,000 Da). The samples were analyzed in a Bio-Rad Imaging scanning densitometer (Versa Dco 3000) with Image Pro Plus 6.0 software. The relative protein quantity of each subunit (protein band) was calculated from its respective percent area against the total area [12].

3.7. Determination of protein concentration

The protein concentration was estimated using the Bradford colorimetric method. To determine the protein concentration, a sample dilution of bovine plasma protein concentrate 1:5 was performed. Then 1 ml of Bradford reagent was added (Coomasie Brillant Blue 250 G, ethanol 95%, phosphoric acid 85%). The detection was done in a spectrophotometer (Shimadzu UV–Visible, double beam) at 595 nm. The protein concentration of samples was determined by comparing the solution absorbance with that of known standards (standard curve of bovine serum albumin, BSA). The concentration was expressed as μg proteins/μl [6].

3.8. Absorption studies

The UV absorption spectra of BPP, with and without $MgCl_2$, was recorder with a spectrophotometer at 190–330 nm at room temperature and physiological pH (7.25 ± 0.05). The concentration of proteins was fixed at 0.1% (w/w).

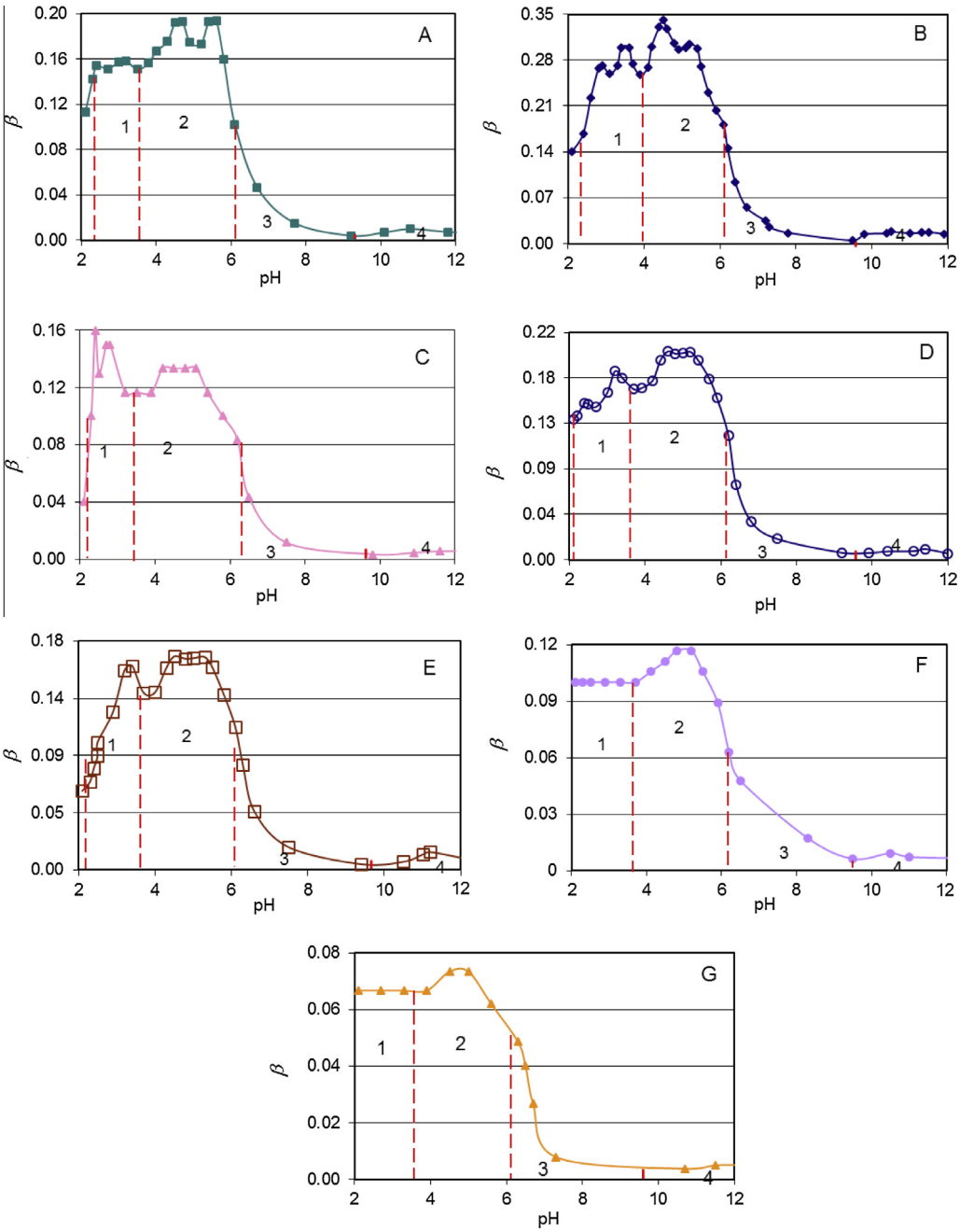

Fig. 4. Buffer capacity (β) of the solutions as a function of pH. Dotted lines indicate the conformational changes of the different solutions prepared with 0.1% (w/v) BPP, $MgCl_2$ and NaCl. A: BPP; B: 0.1% BPP + 0.006% (w/v) $MgCl_2$; C: BPP + 0.02% (w/v) $MgCl_2$; D: BPP + 0.005% (w/v) NaCl; E: BPP + 0.006% (w/v) $MgCl_2$ + 0.005% (w/v) NaCl; F: BPP + 0.006% (w/v) $MgCl_2$ + 0.008% (w/v) NaCl; G: BPP + 0.006% (w/v) $MgCl_2$ + 0.02% (w/v) NaCl.

4. Results and discussion

4.1. Buffer capacity

From the conductometric titration, the buffering capacity of proteins can be evaluated by changing environmental conditions [33] or by adding compounds which may alter its conformational structure, varying hydrodynamic radius [37]. Fig. 3 shows that the curves have a buffering capacity between pH 2.8 and 6.5. Furthermore, adding $MgCl_2$ 0.006% (w/v), a significant increase in the buffering capacity of bovine plasma protein occurred. The addition of $MgCl_2$ at higher concentrations, and in combination with NaCl, caused a reduction in the buffer capacity of proteins. However, adding only 0.05% NaCl (w/v) to the solution of bovine plasma did not produce a statistically significant variation in the buffer capacity.

The variation in the pH buffering capacity is an indication of possible changes in the protein conformations, since all the rearranged the different functional groups of the protein structure change their interaction with the environment [38].

Fig. 1 shows the different protein conformations of BSA versus pH. Analogously, it is possible to determine the different conformations of bovine plasma proteins by varying the pH through the analysis of the protein buffer capacity. Using Eq. (1), the buffer capacity of bovine plasma proteins (0.1% w/v) in the different solutions (control, with NaCl and with $MgCl_2$) was calculated. It should be consider that the BSA is approximately 60% of bovine plasma, yielding a similar profile between the curves of the buffer capacity of bovine plasma and BSA.

In Fig. 4, four conformational transitions were observed, named conformations 1, 2, 3 and 4. When comparing the different solutions of bovine plasma 0.1% (w/v) with the addition of the electrolytes, the buffer capacity of Bovine plasma solution with 0.006% $MgCl_2$ (w/v) presented a statistical significant increase in the buffer capacity between pH 2 and 6, while the buffer capacity of the other solutions resulted unchanged or even decreased.

In Table 2, it is evident that the pH of the different conformations of bovine plasma transitions remained unchanged, except for $MgCl_2$ 0.006% (w/v) in which the pH of the crossover 2 → 3 moves from pH 3.5 to pH 4.0. Something similar – but to a lower extent – was observed with the addition of 0.005% NaCl (w/v) which shifted the transition to pH 3.7. In the solutions in which the $MgCl_2$ (0.006% w/v) and NaCl were combined in different concentrations, that of NaCl increased the displacement produced by $MgCl_2$ at pH 4, moving gradually to pH 3.7 (idem crossover 2 → 3 for NaCl 0.005% w /v).

The peaks for the buffer capacity of the different conformations of the solutions prepared with bovine plasma $MgCl_2$ and NaCl are presented in Fig. 5. A shift in the peaks of bovine plasma solution with the addition of $MgCl_2$ 0.006 and 0.02% (w/v) was observed. The addition of $MgCl_2$ produced a shift to higher pH values in conformation 1 (2.4–2.9 and 3.1–3.5), and a shift toward a lower pH on conformation 2 (4.6–4.5 and 5.5–5.2). Furthermore, the incorporation of NaCl reduced the buffer capacity of the protein, becoming peaks less visible with increasing concentration in the medium. However, the addition of NaCl 0.05% produced virtually no variation in the peaks of the different structures (Table 3).

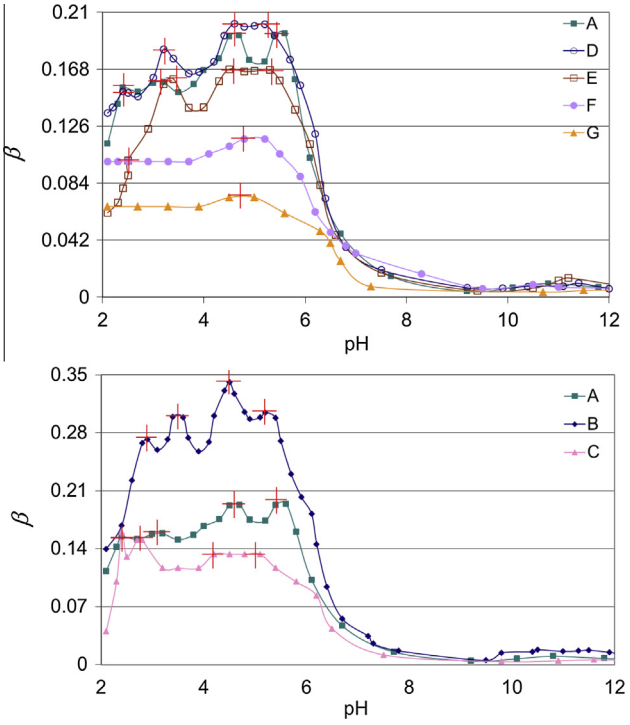

Fig. 5. Maximum peaks of the buffer capacity values (β) conformations of BPP at 0.1% (w/v) prepared with $MgCl_2$ and NaCl at different concentrations. A: BPP; B: BPP + 0.006% (w/v) $MgCl_2$; C: BPP + 0.02% (w/v) $MgCl_2$; D: BPP + 0.005% (w/v) NaCl; E: BPP + 0.006% (w/v) $MgCl_2$ + 0.005% (w/v) NaCl; F: BPP + 0.006% (w/v) $MgCl_2$ + 0.008% (w/v) NaCl; G: BPP + 0.006% (w/v) $MgCl_2$ + 0.02% (w/v) NaCl.

The decreased in buffer capacity of proteins without variation in peak values may be probably due to shielding effect of Na^+ ions, that resulted in weakening of their interaction with the components present in the solution [39].

The higher buffering capacity of bovine plasma solution with the addition of $MgCl_2$ 0.006% (w/v) may be due to a conformational change of the protein, probably because the ion linkage to specific sites within the protein structure modify the internal protein charge generating probably changes in the spatial conformation of the protein. Sadler and Viles [40] demonstrated that albumin possesses binding specific sites for Ca(II). This ion binds to the active sites of the protein resulting in a conformational change by the reduction of the molecule radius. Thus, they can occupy different positions, resulting in the protein net charge and also,

Table 2
Conformational transitions for different BPP solutions with the addition of $MgCl_2$ and NaCl at different concentrations.

Solution % (w/v)	Conformations			
	1 Transition pH	2	3	4
0.1 BPP	2.3 ± 0.1	3.5 ± 0.1	6.1 ± 0.2	9.5 ± 0.1
0.1 BPP + 0.006 $MgCl_2$	2.3 ± 0.1	4.0 ± 0.1	6.1 ± 0.2	9.5 ± 0.2
0.1 BPP + 0.02 $MgCl_2$	2.3 ± 0.2	3.5 ± 0.2	6.1 ± 0.2	9.5 ± 0.3
0.1 BPP + 0.005 NaCl	2.3 ± 0.1	3.7 ± 0.2	6.1 ± 0.1	9.5 ± 0.2
0.1 BPP + 0.006 $MgCl_2$ + 0.005 NaCl	2.5 ± 0.1	3.9 ± 0.2	6.1 ± 0.2	9.5 ± 0.1
0.1 BPP + 0.006 $MgCl_2$ + 0.008 NaCl	–	3.7 ± 0.1	6.1 ± 0.1	9.5 ± 0.2
0.1 BPP + 0.006 $MgCl_2$ + 0.02 NaCl	–	3.7 ± 0.2	6.1 ± 0.1	9.5 ± 0.1

Table 3
Maximum peaks observed in the conformations 1 and 2 for different BPP solutions with $MgCl_2$ and NaCl.

Solution % (w/v)	Conformations			
	1		2	
	pH of the maximum peak			
0.1 BPP	2.4 ± 0.1	3.1 ± 0.1	4.6 ± 0.2	5.5 ± 0.1
0.1 BPP + 0.006 $MgCl_2$	2.9 ± 0.1	3.5 ± 0.2	4.5 ± 0.1	5.2 ± 0.1
0.1 BPP + 0.02 $MgCl_2$	2.4 ± 0.2	2.75 ± 0.12	4.2 ± 0.2	5.1 ± 0.2
0.1 BPP + 0.005 NaCl	2.4 ± 0.1	3.1 ± 0.2	4.6 ± 0.2	5.2 ± 0.1
0.1 BPP + 0.006 $MgCl_2$ + 0.005 NaCl	2.5 ± 0.2	3.4 ± 0.2	4.5 ± 0.1	5.2 ± 0.2
0.1 BPP + 0.006 $MgCl_2$ + 0.008 NaCl	–	–	4.8 ± 0.1[a]	
0.1 BPP + 0.006 $MgCl_2$ + 0.02 NaCl	–	–	4.8 ± 0.1[a]	

[a] The maximum peak value corresponds to the mean value of peaks of conformation 2.

modifying its interaction with the environment. These changes may be related to the functions performed by proteins, as previously explained [38,41]. When the Mg(II) ion is present in the solution at a higher concentration than the Ca(II), the former replaces Ca(II), binding to these active sites. This fact causes a variation of the hydrodynamic radius through conformational changes of the protein [42].

4.2. Influence of different ions in the effective radius or hydrodynamic radius

The hydrodynamic radius of the charged protein increases with the presence of an electric double layer, being its thickness determined from the Debye length by Eq. (8). From this expression, the variation of the Debye length with the pH of the different solutions tested (Table 4) can be evaluated, and the way the pH influences the addition of $MgCl_2$ to the hydrodynamic radius over other salts commonly used, such as NaCl [27], may be observed. In Table 4 can be observed that the values obtained for k_{eff}^{-1} at pH 7.5 for the sample A without addition of salts (3.8 nm) were similar to the values obtained by Wattenbarger et al. [43] for BSA (3.3 nm).

Considering a range of pore diameter between 25 and 50 nm of the membrane and a solute radius of about 4.1 nm (Table 1), from Eqs. (9) and (12), the effective radius r_{eff} (Table 5) and the partition coefficient of the solute ϕ_S can be obtained (Fig. 6) as a function of pH, considering only how influence the effective protein size and the pore size of the membrane in the transmission. Comparing the effective radius of samples BPP 0.1% (w/v) and with the addition of MgCl2 at 0.006% (w/v), we can see that the effective radius decreases significantly from pH 7, this should be because of the union of the Mg ions to the active sites of BSA is pH dependent, with a higher affinity at pH greater than 7 [44].

Fig. 6 shows that a lower transmission of BSA would occur at pH above 7, namely at basic pH due to the increased protein effective size (Table 5). At the pH of the isoelectric point, the protein effective radius is the lowest, and the amount of protein that could pass through the membrane is the highest. This may be due to a shorter length of the electrical double layer (k_{eff}^{-1}, Table 4).

The addition of $MgCl_2$ 0.006% (w/v) leads to an increase of 26% approximately in protein transmission (Fig. 6) between pH 7.0 and 7.5. This may be due to a significant reduction in the effective radius of the proteins (r_{eff}). Fig. 6 also shows that the addition of $MgCl_2$ at a higher concentration would not produce any increase the transmission over a range of pH 7 –7.5, compared with the bovine plasma without salt added. Also, the addition of NaCl 0.005% (w/v) not influenced the transmission at pH between 7 and 7.5 and at a higher pH no variation occurs in the transmission values. Similar results would be achieved by combining $MgCl_2$

Table 4
Variation of the effective Debye letgh of BSA with pH for solutions prepared with 0.1% (w/v) BPP, $MgCl_2$ and NaCl. A: BPP; B: BPP + 0.006% (p/v) $MgCl_2$; C: BPP + 0.02% (w/v) $MgCl_2$; D: BPP + 0.005% (w/v) NaCl; E: BPP + 0.006% $MgCl_2$ + 0.005% (w/v) NaCl; F: BPP + 0.006% (w/v) $MgCl_2$ + 0.02% (w/v) NaCl.

pH	k_{eff}^{-1} (nm)					
	A	B	C	D	E	F
2.0	1.1	1.2	1.5	1.2	1.5	1.5
2.5	1.5	0.9	1.2	1.2	1.3	1.3
3.0	1.1	0.9	1.2	1.0	1.1	1.1
3.5	1.1	0.9	1.3	1.1	1.2	1.2
4.0	1.1	0.8	1.2	1.0	1.1	1.1
4.5	1.1	0.8	1.3	1.0	1.1	1.1
5.0	1.0	0.8	1.1	1.0	1.1	1.1
5.5	1.0	1.0	1.4	1.0	1.2	1.2
6.0	1.7	1.2	1.5	1.4	1.4	1.4
6.5	2.3	1.8	2.9	2.4	2.9	2.9
7.0	3.8	2.6	3.5	3.8	3.4	3.4
7.5	8.6	5.0	7.5	4.3	7.7	7.7
8.0	8.6	7.5	7.9	4.3	7.7	7.7
8.5	8.6	7.9	7.9	4.3	7.7	7.7
9.0	6.7	7.9	7.9	4.7	7.7	7.7
9.5	6.7	4.2	6.1	4.6	5.3	5.3
10.0	3.5	3.4	6.7	5.0	5.7	5.7
10.5	4.8	4.8	3.0	5.7	4.8	4.8
11.0	4.8	3.4	3.0	4.2	3.7	3.7
11.5	6.7	4.8	3.0	5.0	4.5	4.5
12.0	1.1	1.2	1.5	1.2	1.5	1.5

Table 5
Variation of the effective radius of BSA with pH for solutions prepared with 0.1% (w/v) BPP, $MgCl_2$ and NaCl. A: BPP; B: BPP + 0.006% (w/v) $MgCl_2$; C: BPP + 0.02% (w/v) $MgCl_2$; D: BPP + 0.005% (w/v) NaCl; E: BPP + 0.006% $MgCl_2$ + 0.005% (w/v) NaCl; F: BPP + 0.006% (w/v) $MgCl_2$ + 0.02% (w/v) NaCl.

pH	r_{eff} (nm)					
	A	B	C	D	E	F
2.0	23.2	24.8	29.4	24.8	29.4	35.0
2.5	19.7	13.5	17.3	17.3	18.1	20.3
3.0	10.5	9.4	11.5	10.1	10.5	15.3
3.5	7.0	6.4	7.6	7.0	7.2	8.5
4.0	4.8	4.6	4.9	4.8	4.8	5.2
4.5	4.1	4.1	4.1	4.1	4.1	4.1
5.0	4.2	4.2	4.2	4.2	4.2	4.3
5.5	4.5	4.5	4.7	4.6	4.6	7.5
6.0	5.8	5.3	5.7	5.6	5.5	5.5
6.5	8.4	7.4	9.3	8.4	9.3	9.2
7.0	14.9	11.5	14.0	14.9	13.8	17.1
7.5	39.5	24.7	34.7	21.7	35.7	37.7
8.0	52.3	45.8	48.5	28.0	47.1	49.8
8.5	67.1	62.1	62.1	35.4	60.3	53.7
9.0	66.3	77.6	77.6	47.4	75.3	61.7
9.5	80.9	51.9	74.0	56.1	64.8	65.2
10.0	52.1	50.8	96.5	73.6	82.5	83.5
10.5	82.7	82.5	53.9	97.8	82.5	76.7
11.0	96.3	69.4	62.5	85.1	74.9	88.9
11.5	154.5	110.8	71.9	365.7	105.9	150.0
12.0	23.2	24.8	29.4	24.8	29.4	35.0

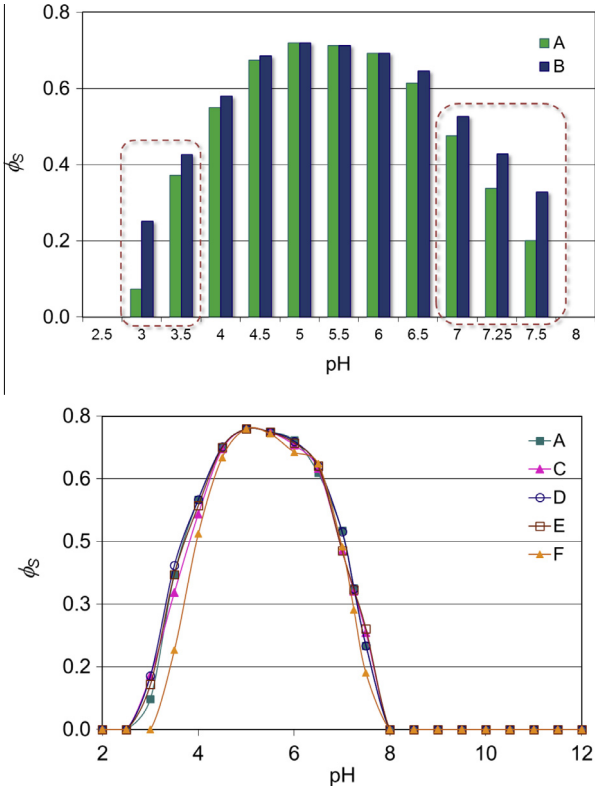

Fig. 6. Variation of the partition coefficient (ϕ_S) of BSA with pH for different solutions 0.1% (w/v) BPP and $MgCl_2$. A: BPP; B: BPP + 0.006% (w/v) $MgCl_2$; C: BPP + 0.02% (w/v) $MgCl_2$; D: BPP + 0.005% (w/v) NaCl; E: BPP + 0.006% $MgCl_2$ + 0.005% (w/v) NaCl; F: BPP + 0.006% (w/v) $MgCl_2$ + 0.02% (w/v) NaCl.

(0.006% w/v) and NaCl 0.005% (w/v) and at higher concentrations of NaCl (0.02% w/v) with constant concentration of $MgCl_2$ (0.006%, w/v).

4.3. Determination of resistances

From the experimental data of filtration experiences with deionized water, and by plotting the permeate flux density versus transmembrane pressure, the hydraulic permeability of the membrane was obtained (Eq. (13)): 0.08 L m^{-2} h^{-1} bar^{-1}.

By plotting the data of permeate flux (J) versus transmembrane pressure (ΔP) for deionized water at a temperature of 25 ± 1 °C, the intrinsic resistance of the membrane can be obtained from Eq. (14), considering $R_S = 0$: $R_M = 1.25 \times 10^6$ m^{-1}.

Fig. 7 shows the data obtained from the permeate flux versus transmembrane pressure for the different feed solutions of bovine plasma with different concentrations of $MgCl_2$ (0%, 0.006% and 0.02%, w/v), at constant temperature. It can be observed a typical behavior in which the permeate flux increased with an increasing transmembrane pressure; however, due to the formation of a concentration polarization layer, a limiting concentration was reached, so then, the permeate flux became independent of pressure. Thus, the selected pressure was 1.2 bar for all the experiences. Fig. 7 show that the highest permeate flux was obtained for the solution of bovine plasma with $MgCl_2$ (0.006% (w/v)). This behavior could be explained by the fact that Mg ions bind to the BSA binding sites modifying the net protein charge and, also, their interaction with the membrane and the environment.

From the data of permeate flux, transmembrane pressure, the membrane resistance, and the viscosity of the permeate solution (μ = 1.3 g/cm s), R_S can be evaluated (Eq. (14)). From the fitting

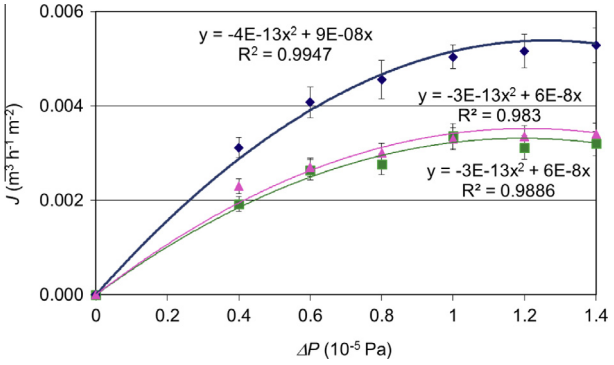

Fig. 7. Permeate flux density versus transmembrane pressure for different feed solutions with 0.1% (w/v) BPP: (A) BPP; (B) BPP + 0.006% (w/v) $MgCl_2$; (C) BPP + 0.02% (w/v) $MgCl_2$ (T = 25 ± 1 °C).

Table 6
Values of R_F, R_P, R_S and the percent error between theoretical and experimental values obtained from series resistance model: (A) 0.1% (w/v) BPP; (B) 0.1% (w/v) BPP + 0.006% (w/v) $MgCl_2$; (C) 0.1% (w/v) BPP + 0.02% (w/v) $MgCl_2$. (ΔP = 1.2 bar; T = 25 ± 1 °C). The percentage error calculated for the experimental data correspond with the 5%.

Feed solution	$MgCl_2$ (% w/v)	R_F (m^{-1})	α	R_P (m^{-1})	Percent error (%)	R_S (m^{-1})
A	0	6×10^7	2053.5	2.46×10^8	7.2 ± 2.0	2.95×10^8
B	0.006	5×10^7	1059.6	1.27×10^8	2.2 ± 0.7	1.78×10^8
C	0.02	6×10^7	1795.1	2.15×10^8	1.1 ± 0.4	2.74×10^8

curve (Eq. (18)), R_F and α were obtained, and are listed in Table 6. The theoretical equations that characterize the permeate flux through the membrane may be obtained by these variables. Table 6 shows that the proposed model adequately fits the experimental data, being the percentage error less than 10%.

Considering the resistances due to the fouling of the solute (R_S), it can be observed that the lowest value corresponds to the solution of plasma with $MgCl_2$ 0.006% (w/v). This behavior suggests that, in effect, the protein has the highest net charge with a higher buffer capacity, or the effective charge was changed due to the bind of Mg^{2+} ions to specific binding sites of BSA, generating more rejection among protein molecules and a decreasing in protein aggregation or a lower absorption of the proteins on the membrane surface. Consequently, it results in a less compact layer polarization in the membrane (Fig. 7). These results are in agreement with those found by de la Casa et al. [3] and Ibañez et al. [36]. Ibañez et al. found that when the proteins present a higher net charge as at extreme pHs, the repulsion among the molecules yield minimum values of R_S. Besides, de la Casa et al. [3] describes that changes in the net charge of the protein or membrane reduce de protein aggregation or the absorption on membrane surface decreasing the fouling resistance.

4.4. Determination of the protein concentration for permeate and retentate streams

Table 7 shows that a maximum experimental protein transmission was obtained for the solution of plasma bovine with $MgCl_2$ 0.006% (w/v), which is in accord with the theoretical BSA transmission ($T_{r\phi}$). Table 7 also shows the experimental relative error (E_{rexp}), which represent the difference from the theoretical value. The results confirmed the model effectiveness to predict the transfer in complex dilute solutions. This behavior could be explained by the minimum effective radius of the protein molecules, as previously discussed. This is consistent with the results obtained by

Table 7
Protein concentration and transmission of BPP 0.1% (w/v) with and without the addition of different concentrations of $MgCl_2$: (A) 0% (w/v); (B) 0.006% (w/v); (C) 0.02% (w/v) at pH = 7.25 ± 0.05 (ΔP = 1.2 bar; T = 25 ± 1 °C; VCR = 1.15 ± 0.05).

Solutions	Streams	Protein concentration (μg/μL)	T_r (%)	$T_{r\phi}$ (%)	E_{rexp} (%)
A	Retentate	0.70 ± 0.05	32.6 ± 2.3	33.8	3.6
	Permeate	0.42 ± 0.04			
B	Retentate	0.67 ± 0.04	41.8 ± 2.9	42.7	2.2
	Permeate	0.62 ± 0.05			
C	Retentate	0.71 ± 0.06	33.7 ± 2.7	33.0	−2.1
	Permeate	0.45 ± 0.05			

Ibañez et al. [36] and de la Casa et al. [27], who studied the evolution and transmission of β-lactoglobulin Lysozyme and BSA, respectively, as a function of pH. They found that, at the pH at which the effective radius was smaller, the protein transmission increased considerably.

4.5. Analyses of the proteins present in each stream

The feed solution of plasma with $MgCl_2$ 0.006% (w/v), as well as the permeate and retentate were analyzed. The SDS–PAGE for all the samples is presented in Fig. 8, where M corresponds to molecular weight marker, while wells 1 and 2 correspond to the permeate and retentate from bovine plasma without the addition of salt. In wells 3 and 4 the permeate and retentate of the solution with $MgCl_2$, 0.006% (w/v) are presented, and in well 5, the feed solution.

From the results obtained, the majority protein, BSA, was easily identified (66 kDa band). Furthermore, considering Table 1, it is observed that 59 kDa band corresponds to α_1-globulins.

Using the Image Pro Plus 6.0 software, the area of each of the bands detected in the SDS–PAGE gel was calculated. Thus, comparing the experiences with and without salt added, a decrease of ≈18% in the band area of BSA in well 4 (retentate of bovine plasma + $MgCl_2$ 0.006%), and an increase in the band area in 3 (≈24%) (permeate with $MgCl_2$) were distinguished. These results are consistent with the increase obtained in the protein transmission of about 25% (Table 7).

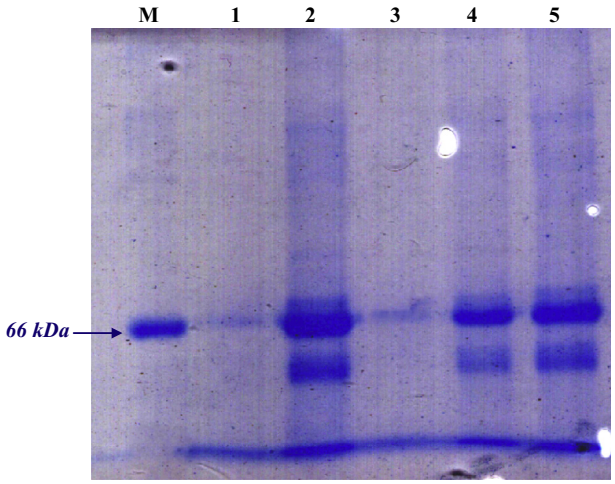

Fig. 8. Polyacrylamide gel electrophoresis of the solutions of 0.1% (w/v) bovine plasma with and without the addition of 0.006% (w/v) $MgCl_2$. Revealed by staining with Coomassie Brillant Blue. Wells: M = molecular weight marker; 1 and 2 = permeate and retentate of BPP; 3 and 4 = permeate and retentate of BPP + 0.006% (w/v) $MgCl_2$; 5 = feed solution, BPP.

4.6. Binding studies using UV absorption spectra

A UV–Vis absorption measurement is a simple but effective method for detecting complex formation and confirming the probable changes in protein conformation, even at the low concentrations that are typical of physiological conditions [38,39].

Serum albumins have many physiological functions. It aids in the transport, distribution and metabolism of many endogenous and exogenous compounds, including binding to fatty acids, amino acids, metal ion and others compounds [45,46]. The sites available in BSA for the binding of Ca(II) include 16 imidazole groups and 56 amino groups as well approximately one hundred carboxylate ions and the increase of pH generates increase in the possibility of calcium binding to BSA. This increase has generally been attributed to electrostatic effects, obtaining a greater affinity between pH 7 and 10 [47].

The absorption spectrum of BSA has a maximum absorption band at 280 nm and a higher maximum at 210 nm. The first is related to electron transition ($\rightarrow \pi^*$) of π bonds of aromatic amino acids of tyrosine, phenyl alanine and tryptophan and the latter is related to transition ($\pi \rightarrow \pi^*$) of amide groups of peptide bonds [45]. Therefore, the band at 280 nm corresponds to binding groups of Ca(II) as was previously described.

Fig. 9 shows the variation of intensity valor of absorption at 210 nm (BSA higher absorption peak) for different concentration of $MgCl_2$ in the range studied. An important change in the absorption n the spectra can be observed for range comprised between 0.004% and 0.008% (w/v) of $MgCl_2$, which is in accord to the concentration at which changes in behavior BSA were observed (0.006% w/v).

The UV spectra for BPP in presence and absence of Mg(II) at physiological pH (7.25 ± 0.05) is shown in Fig. 10. The curves show two bands: one around 210 nm and the other at 280 nm. It is noteworthy that the absorption around 210 nm increases with the incorporation of $MgCl_2$ at 0.006% (w/v), while for the spectra of the other solutions remained unchanged with respect to the sample of BPP 0.1% (w/v). As the absorption peaks at 210 and 280 nm correlated with specific functional groups transition, which correspond to the binding sites of the Ca^{2+} and Mg^{2+} ions [42]. Therefore, it is possible to observe changes in protein conformation from the changes observed in the peak intensity of the UV spectrum, as was exposed. Liang et al. [21] and Yongqia et al. [22] studied the interactions of Ni(II) and Co(II), with bovine serum albumin, respectively. These authors also observed a hyperchromic effect in the spectra for the linkage of the ion with BSA in the concentration range between 1 and 4×10^{-4} M. Furthermore, the absorption peaks at 280 and 210 had not blue shift. Besides, UV spectra of BPP-Mg(II) at 1 h of preparation (Fig. 10) present an increase of 14% in the area of band at 210 nm with respect to BPP, while the

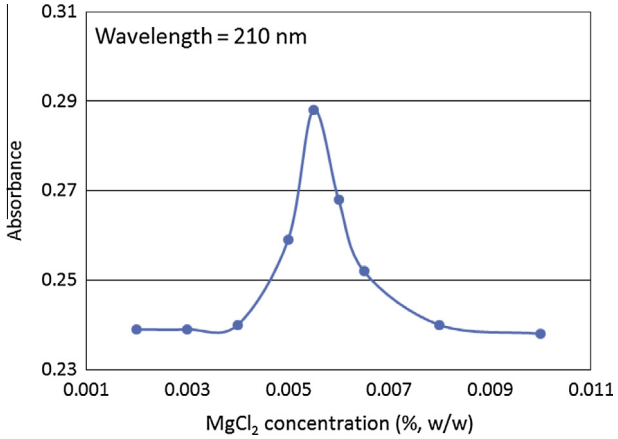

Fig. 9. UV absorption at 210 nm for Mg(II)-BPP system at different concentrations.

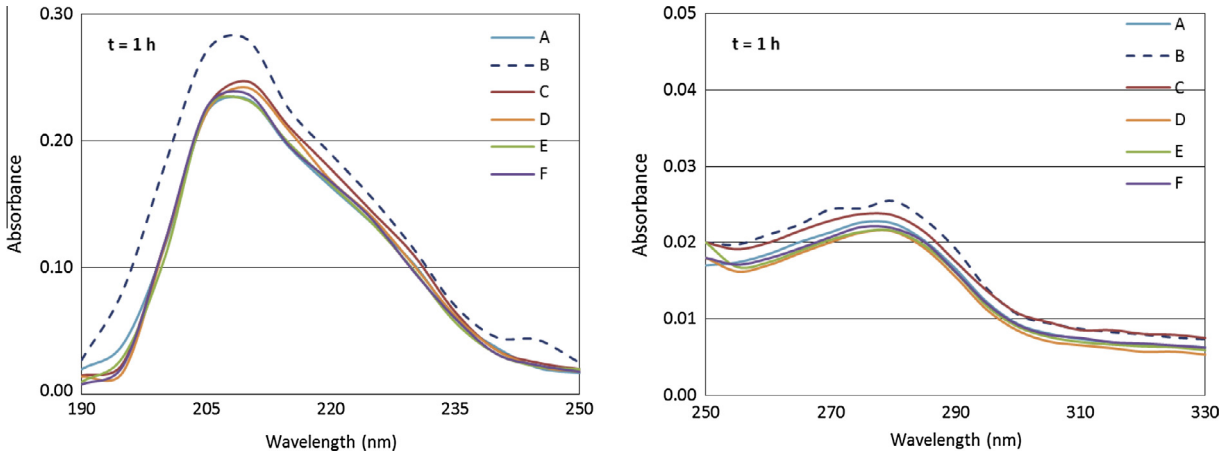

Fig. 10. UV-absorption spectra of BPP at 0.1% (w/v) with and without combinations of $MgCl_2$ and NaCl. A: BPP; B: BPP + 0.006% (w/v) $MgCl_2$; C: BPP + 0.02% (w/v) $MgCl_2$; D: BPP + 0.005% (w/v) NaCl; E: BPP + 0.006% $MgCl_2$ + 0.005% (w/v) NaCl; F: BPP + 0.006% (w/v) $MgCl_2$ + 0.02% (w/v) NaCl.

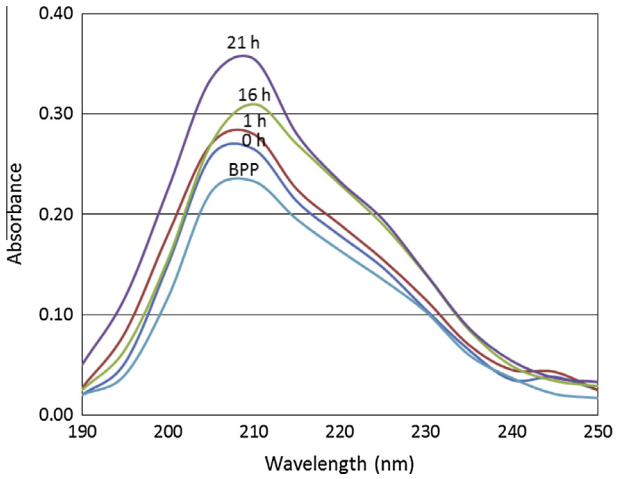

Fig. 11. Time-scanning UV spectra (numbers on curves indicate time (h)) for the systems BPP at 0.1% (w/v) and BPP + 0.006% (w/v) $MgCl_2$.

area of band at 280 nm remains unchanged. As was previously described, organic macromolecules that contain carboxyl and/or amino groups absorbed below 220 nm. Furthermore, BSA usually acts as sequestration agent of metal ions, being reasonable that metal ions would bind to BSA [48]. These observations strongly support the postulate that the binding of BPP with Mg(II) in the site available for the binding with Ca(II) may cause a conformational change in BSA. The phenomenon of molecular conformational changes caused by metal ions-BSA binding was previously observed by the binding of Co(II) to BSA studied by Liang et al. [21].

Fig. 11 shows the variation in time of greater absorption peak (210 nm) of BSA bound to Mg ions to a concentration of 0.006% (w/v). In the same manner, the results obtained by Yongqia et al. [22] for the study of the BSA and HSA linked to Ni(II) ions, where a significant increase in the peak values with time can be observed. This may be due to the existence of multiple binding sites of Mg(II), so probably after the binding of first Mg(II) ions, an induced conformational transition happened, which leaded to the binding of the subsequent ions. Similar results were presented by Yongqia et al. [22].

5. Conclusions

Considering the molecular size of the different proteins that form the plasma and the Debye length, or formation of electric double layer that significant increases the protein radio (working outside the range of the isoelectric point of the protein) all the proteins would be largely retained and, therefore, concentrated without selectivity during the permeation experience. Based on this principle, the effect of different salts (electrolytes) on conformational changes in the protein, determining changes in size was investigated. Thus, the effect of $MgCl_2$ concentration on the permeate flux, and of the transmission of plasma through a ceramic UF membrane proteins was examined. The changes observed in the buffer capacity of the proteins showed the existence of conformational changes by the addition of $MgCl_2$. The protein hydrodynamic radius was evaluated by using the Debye equation. It was noted that a significant reduction in this parameter may be due to the addition of $MgCl_2$ 0.006% (w/v). The studies of protein concentration and identification by gel electrophoresis suggest that the addition of $MgCl_2$ 0.006% (w/v) produces an increase of about 25% protein transmission because of conformational changes that generate a decrease in the hydrodynamic radius. This result was confirmed by the UV spectra performed. Furthermore, from the calculation of the system resistances, using the model of resistances in series, a significant decrease in the solute (R_S) resistance due to the addition of $MgCl_2$ 0.006% (w/v) was observed. This behavior could be explained by the fact that the binding of Mg (II) to the specific sites of BSA modify the net protein charge and, therefore, induced conformational changes and changes the interaction with the membrane and the environment.

Further research could be done at lower pH, in which the highest values of partition coefficient was obtained, along with the results obtained in this work, and improve in membrane separative efficiency can be reached.

Acknowledgments

Financial support provided by the SCyT, UNSL (Project 22Q/011) and PICT 2012-0155 (ANPCyT), also fellowships of Dra. Laura Rodriguez Furlán of the CONICET (Argentina) are gratefully acknowledged.

References

[1] A. Saxena, B.P. Tripathi, K. Mahendra, V.K. Shahi, Membrane-based techniques for the separation and purification of proteins: an overview, Adv. Colloid Interface 145 (2009) 1–22.
[2] L. Ricq, A. Pierre, J.C. Reggiani, S. Zaragoza-Piqueras, J. Pagetti, G. Daufin, Effects of proteins on electrokinetic properties of inorganic membranes during ultra- and micro-filtration, J. Membr. Sci. 114 (1996) 27–38.
[3] E.J. de la Casa, A. Guadix, R. Ibáñez, E.M. Guadix, Influence of pH and salt concentration on the cross-flow microfiltration of BSA through a ceramic membrane, Biochem. Eng. J. 33 (2007) 110–115.

[4] M.C. Almécija, R. Ibáñez, A. Guadix, E.M. Guadix, Effect of pH on the fractionation of whey proteins with a ceramic ultrafiltration membrane, J. Membr. Sci. 288 (2007) 28–35.
[5] M. Rabiller Baudry, B. Chaufer, D. Lucas, F. Michel, Ultrafiltration of mixed protein solutions of lysozyme and lactoferr: role of modified inorganic membranes and ionic strength on the selectivity, J. Membr. Sci. 184 (2001) 137–148.
[6] E. Darnon, E. Morin, M.P. Belleville, G.M. Rios, Ultrafiltration within downstream processing: some process design considerations, Chem. Eng. Process. 42 (2003) 299–309.
[7] D. Lucas, M. Rabiller-Baudry, F. Michel, B. Chaufer, Role of the physico-chemical environment on ultrafiltration of lysozyme with modified inorganic membrane, Colloids Surf. A 136 (1998) 109–122.
[8] M. Diná Afonso, R. Bórquez, Review of the treatment of seafood processing wastewaters and recovery of proteins therein by membrane separation processes-prospects of the ultrafiltration of wastewaters from the fish meal industry, Desalination 142 (2002) 29–45.
[9] M.A. Argüello, S. Álvarez, F.A. Riera, R. Álvarez, Enzymatic cleaning of inorganic ultrafiltration membranes used for whey protein fractionation, J. Membr. Sci. 216 (2003) 121–134.
[10] M.A. Argüello, S. Álvarez, F.A. Riera, R. Álvarez, Utilization of enzymatic detergents to clean inorganic membranes fouled by whey proteins, Sep. Purif. Technol. 41 (2005) 147–154.
[11] P. Pedraz, J. Cortés, O. Hilgendorf, S. Rassid, C. Bogaert, O. Herouard, F.J. Montes, M.E. Díaz, R.L. Cerro, Affinity separation by Langmuir-Blodgett deposition of bovine serum albumin using arachidic acid as specific ligand, Sep. Purif. Technol. 143 (2015) 161–168.
[12] B.E. Chove, A.S. Grandison, M.J. Lewis, Some functional properties of fractionated soy protein isolates obtained by microfiltration, Food Hydrocolloids 21 (2007) 1379–1388.
[13] K. Mueller, P. Eisner, Y. Yoshie-Stark, R. Nakada, E. Kirchhoff, Functional properties and chemical composition of fractionated brown and yellow linseed meal (Linum usitatissimum L.), J. Food Eng. 98 (4) (2010) 453–460.
[14] F. Jahaniaval, Y. Kakuda, V. Abraham, M.F. Marcone, Soluble protein fractions from pH and heat treated sodium caseinate: physicochemical and functional properties, Food Res. Int. 33 (2000) 637–647.
[15] J.D. Sarma, C. Duttagupta, E. Ali, T.K. Dhar, Antibody to folic acid: increased specificity and sensitivity in ELISA by using ε-aminocaproic acid modified BSA as the carrier protein, J. Immunol. Methods 184 (1995) 1–6.
[16] I. Jacques, V. Olivier-Bernardin, G. Dubray, Induction of antibody and protective responses in mice by Brucella O-polysaccharide-BSA conjugate, Vaccine 9 (12) (1991) 896–900.
[17] G.L. Francis, Albumin and mammalian cell culture: implications for biotechnology applications, Cytotechnology 62 (2010) 1–16.
[18] W. Catteral, Functional subunit structure of voltage-gated calcium channels, Science 253 (1991) 1499–1500.
[19] C. Heizmann, W. Hunziker, Intracellular calcium-binding proteins: more sites than insights, Trends Biochem. Sci. 16 (1991) 98–103.
[20] M. Mayre, E. Miller, Excitatory aminoacid receptors, second messengers and regulation of intracellular Ca^{2+} in mammalian neurons, Trends Pharmacol. Sci. 11 (1980) 254–260.
[21] H. Liang, Jin Huang, Chu-Qiao Tu, Min Zhana, Yong-Qia Zhou, Pan-Wen Shen, The subsequent effect of interaction between Co^{2+} and human serum albumin or bovine serum albumin, J. Inorg. Biochem. 85 (2001) 167–171.
[22] Z. Yongqia, H. Xuying, O. Di, H. Jiesheng, W. Yuwen, Research communication. The novel behavior of interactions between Ni^{2+} ion and human or bovine serum albumin, Biochem. J. 304 (1994) 23–26.
[23] K. Nakamura, S. Era, Y. Ozaki, M. Sogami, T. Hayashi, M. Murakami, Conformational changes in seventeen cystine disulfide bridges of bovine serum albumin proved by Raman spectroscopy, FEBS Lett. 417 (1997) 375–378.
[24] M.L. Ferrer, R. Duchowicz, B. Carrasco, J. Garcia de la Torre, U. Acuña, The conformation of serum albumin in solution: a combined phosphorescence depolarization-hydrodynamic modeling study, Biophys. J. 80 (2001) 2422–2430.
[25] C.T. Lee, Kenneth A. Smith Jr., T. Alan Hatton, Photocontrol of protein folding: the interaction of photosensitive surfactants with bovine serum albumin, Biochemistry 44 (2005) 524–536.
[26] R.A. Curvale, Buffer capacity of bovine serum albumin (BSA), J. Argent. Chem. Soc. 97 (2009) 174–180.
[27] E.J. de la Casa, A. Guadix, R. Ibáñez, F. Camacho, E.M. Guadix, A combined fouling model to describe the influence of the electrostatic environment on the cross-flow microfiltration of BSA, J. Membr. Sci. 318 (2008) 247–254.
[28] R. Tadmor, E. Hernández Zapat, N. Chen, P. Pincus, J.N. Israelachvili, Debye length and double-layer forces in polyelectrolyte solutions, Macromolecules 35 (2002) 2380–2388.
[29] N.S. Pujar, A.L. Zydney, Electrostatic effects on protein partitioning in size exclusion chromatography and membrane ultrafiltration, J. Chromatogr. A 796 (1998) 229–232.
[30] P. Perrona, L. Sever, Method for Filtering a Three-phased Reaction Mixture, United States Patent. Patent N°: US 6,478,968 B1, 2002.
[31] F.G. Smith, W.M. Deen, Electrostatic double-layer interactions for spherical colloids in cylindrical pores, J. Colloid Interface Sci. 78 (1980) 444–465.
[32] S. Kaliappan, J.A. Lucey, Influence of mixtures of calcium-chelating salts on the physicochemical properties of casein micelles, J. Dairy Sci. 94 (9) (2011) 4255–4263.
[33] M. Nyström, P. Aimar, S. Luque, M. Kulovaara, S. Metsamuuronen, Fractionation of model proteins using their physiochemical properties, Colloids Surf. A 138 (1998) 185–205.
[34] A.D. Marshall, P.A. Munro, G. Trägardh, The effect of protein fouling in microfiltration and ultrafiltration on permeate flux, protein retention and selectivity: a literature review, Desalination 91 (1993) 65.
[35] M. Cheryan, Ultrafiltration and Microfiltration Handbook, Technomic Publishing Co., Inc., Lancaster, 1998.
[36] R. Ibañez, M.C. Almécija, A. Guadix, E.M. Guadix, Dynamics of the ceramic ultrafiltration of model proteins with different isoelectric point: comparison of β-lactoglobulin and lysozyme, Sep. Purif. Technol. 57 (2007) 314–320.
[37] L. Millesime, Role des interactions sur la retention de proteins par des membranes ́ultrafiltration. Cas particulier de membranes modifiees par depot de polymeres quaternises, Ph.D. Thesis, Université Paris VI, 1993.
[38] R.S. Mani, C.M. Kay, Hydrodynamic properties of bovine brain S-100 proteins, FEBS 166 (2) (1984) 258–262.
[39] T. Hianik, V. Ostatná, M. Sonlajtnerov, I. Grman, Influence of ionic strength, pH and aptamer configuration for binding affinity to thrombin, Bioelectrochemistry 70 (2007) 127–133.
[40] P.J. Sadler, J.H. Viles, ^{1}H and ^{113}Cd NMR investigations of Cd^{2+} and Zn^{2+} binding sites on serum albumin: competition with Ca^{2+}, Ni^{2+}, Cu^{2+}, and Zn^{2+}, Inorg. Chem. 35 (1996) 4490–4496.
[41] J. Baudier, R.D. Cole, The Ca^{2+}-binding sequence in bovine brain S100b protein β-subunidad, Biochem. J. 264 (1989) 79–85.
[42] C.A. Builes Barrera, R. Gómez Wolff, G. Latorre Sierra, C.H. Morales Uribe, J.J. Orrego Beltrán, A. Orrego Monsalve, Endocrinología, in: A. Orrego Monsalve (Ed.), Editorial Universidad de Antioquía, second ed., Colombia, 2009, pp. 139.
[43] M.R. Wattenbarger, V.A. Bloomfield, Tracer diffusion of proteins in DNA solutions, Macromolecules 25 (1992) 5263–5265.
[44] F. Casanueva Freijo, J.A. Vazquez Garcia, S. Gaztambide Sáenz, Endocrinología Clínica, Ed. Diaz de Santos, Argentina, 1995, pp. 120.
[45] N. Shahabadi, A. Khorshidi, M. Mohammadpour, Investigation of the effects of Zn^{2+}, Ca^{2+} and Na^{+} ions on the interaction between zonisamide and human serum albumin (HSA) by spectroscopic methods, Spectrochim. Acta A 122 (2014) 48–54.
[46] J. Zhang, L. Chen, B. Zeng, Q. Kang, L. Dai, Study on the binding of chloroamphenicol with bovine serum albumin by fluorescence and UV–vis spectroscopy, Spectrochim. Acta A 105 (2013) 74–79.
[47] H.A. Saroff, M.S. Lewis, The binding of calcium ions to serum albumin, J. Phys. Chem. 67 (6) (1963) 1211–1216.
[48] Xue-Feng Liu, Yong-Mei Xia, Yun Fang, Effect of metal ions on the interaction between bovine serum albumin and berberine chloride extracted from a traditional Chinese Herb coptis chinensis franch, J. Inorg. Biochem. 99 (2005) 1449–1457.